Russian Chemical Reviews **67** (2) 109 – 122 (1998) © 1998 Russian Academy of Sciences and Turpion Ltd

UDC 541.18, 548.3

Chemistry of semiconductor nanoparticles

R F Khairutdinov

Contents

I.	Introduction	109
II.	Methods for the synthesis of nanoparticles	110
III.	The quantum size effects	112
IV.	Photocatalytic processes with the participation of semiconductor nanostructures	117
V.	Conclusion	119

Abstract. Basic advances and prospects of further research in the field of the chemistry of nanoparticles are considered. The principal factors determining the unusual physicochemical properties of semiconductor nanoparticles are discussed. It is pointed out that the kinetics of chemical transformations on the surface and in the bulk of nanoparticles differs from that in infinite space. The classical equations of chemical kinetics can be used for the description of the processes on the surface of nanoparticles down to a size that exceeds the size of the reacting molecules by an order of magnitude. The large relative fraction of surface atoms in nanoparticles determines the size dependences of the melting temperature and pressure at which the crystal lattice of a semiconductor rearranges (*i.e.*, a phase transition occurs in the semiconductor crystal). Because of the comparable size of nanoparticles and the delocalisation radii of charge carriers nonlinear optical effects arise and the redox properties and optical characteristics of nanoparticles become dependent on their size. The bibliography includes 219 references.

I. Introduction

It is usually assumed that the properties of solid semiconductors are independent of their size. However, this assumption is only valid for the solids containing a macroscopic number of atoms. Recent studies have shown that if the characteristic size of semiconductor particles is less than 10 nm, then many of their physicochemical properties appear to be essentially different from analogous properties of macroscopic objects. This is related to the fact that semiconductors are characterised by high energies of intermolecular interactions and a macroscopic crystal can be considered as one large molecule when its electronic properties are described. The electronic excitation of semiconductor crystals results in the formation of a loosely coupled electron – hole pair. In semiconductors, the size of the delocalisation area of such a pair can be many times larger than the lattice constant. The decrease in the size of a semiconductor crystal down to a size comparable with the delocalisation area of the electron – hole pair affects its electronic characteristics. The blue shift of the excitonic absorption band of a semiconductor crystal with decreasing its size is a remarkable manifestation of this effect.[1–3] For CdS, which is the best studied semiconductor material, the blue shift of the excitonic absorption band is observed beginning from a crystal size of 5 – 6 nm. Ultrasmall semiconductor crystals are known in the literature as nanocrystals, particles with quantum size effect, or nanoparticles. The intensive studies of physicochemical properties of nanocrystals that have been carried out during the last decade have revealed a large number of other their unusual characteristics, such as the size dependence of the radiative lifetime of the electronic excitation, melting temperature, pressure needed for the rearrangement of the crystal structure (*i.e.*, for a phase transition to occur in the crystal), and character of the kinetics of chemical processes on the surface of nanoparticles.

Unusual physicochemical properties of nanoparticles are due to three main reasons. First, as has been noted above, the size of nanoparticles is comparable to the Bohr radius of the excitons in semiconductors. This determines the optical, luminescent, and redox properties of nanoparticles. Second, the surface atoms constitute a considerable fraction of the total number of the atoms of the nanoparticle. For example, a 5-nm CdS nanocrystal has about 15% of the atoms on the surface. The surface atoms contribute largely to the thermodynamic characteristics of solids and determine to a considerable extent the melting temperature and structural transitions for nanoparticles. Third, the natural size of the nanoparticles is comparable with the size of molecules. This determines the peculiarities of the kinetics of chemical processes on the surface of nanoparticles.

Most of the studies of semiconductor nanoparticles are of interdisciplinary character and are devoted to investigation of their colloidal solutions. To date, nanoparticles of ZnO, Fe_2O_3, SiO_2, MoS_2, CdS, HgS, GaP, Cd_3P_2, BiI_3, PbI_2, and a number of other semiconductors have been synthesised and investigated. For several semiconductor nanoparticles, the structure of the electronic bands and electrochemical characteristics, optical properties and photochemical reactions, processes of charge separation and recombination, mechanical and thermal properties, regularities of reactions of the molecules adsorbed on the surface have been investigated.

In this review, the major achievements in the chemistry of semiconductor nanoparticles are considered. Methods for the synthesis of nanoparticles, quantum size effects characteristic of semiconductor nanoparticles, photocatalytic processes with participation of semiconductor nanoparticles and films prepared on their base are considered. The primary attention is given to the prospects of the use of the nanostructures to implement practically important processes of photomineralisation of environmentally

R F Khairutdinov N N Semenov Institute of Chemical Physics, Russian Academy of Sciences, ul. Kosygina 4, 117977 Moscow, Russian Federation. Fax (7-095) 938 21 56. Tel. (7-095) 939 74 85.
E-mail: rafail@center.chph.ras.ru

Received 6 February 1997
Uspekhi Khimii **67** (2) 125 – 139 (1998); translated by A M Raevsky

hazardous organic compounds. In the concluding section of this review, a brief outline of feasible lines for further development of nanochemistry is given.

II. Methods for the synthesis of nanoparticles

Methods for the synthesis of nanoparticles can be divided into three main groups.

1. Synthesis of semiconductor nanoparticles in solutions of the corresponding salts by controlled addition of anions (or cations) or by hydrolysis.[4–19]

2. Preparation of nanoparticles as a result of phase transformations.[20–22]

3. The synthesis of nanoparticles in aerosols.[23–25]

The radiation-chemical method for the synthesis of nanoparticles is also known.[3] Methods for the synthesis of complex multicomponent nanoparticles have been developed. Most of the semiconductor colloidal systems studied to date have been obtained by synthesising the semiconductor nanoparticles in homogeneous solution.

Commercial colloidal solutions containing the SnO_2 nanoparticles (with an average diameter of 3 nm) are available from Johnson Matthey (USA). A Degussa P25 TiO_2 powder containing 80% of anatase and 20% of rutile is often used in photocatalysis.[26]

1. Synthesis of semiconductor nanoparticles in colloidal solutions

The semiconductor nanoparticles are prepared by chemical synthesis in homogeneous solutions,[4–7] in micelles, vesicles, and Langmuir–Blodgett films,[8–11, 27, 28] in polymers,[12–14] in glasses,[15, 16] in zeolites,[17–19] and in β-cyclodextrin.[29]

The easiest and most common method for the preparation of semiconductor nanoparticles is the synthesis from the starting reagents in solution by arresting the reaction at a definite moment.[4–7] Nanoparticles of metal sulfides are synthesised by a reaction of a water-soluble metal salt and H_2S (or Na_2S) in the presence of an appropriate stabiliser such as sodium metaphosphate. For example, the CdS nanoparticles can be synthesised by mixing $Cd(ClO_4)_2$ and Na_2S solutions:

$$Cd(ClO_4)_2 + Na_2S = CdS\downarrow + 2NaClO_4 . \quad (1)$$

The growth of the CdS nanoparticles in the course of reaction is arrested by an abrupt increase in pH of the solution.

Colloidal particles of metal oxides can be obtained by hydrolysis of the corresponding salts. For example, the TiO_2 nanoparticles are readily formed in the hydrolysis of titanium tetrachloride

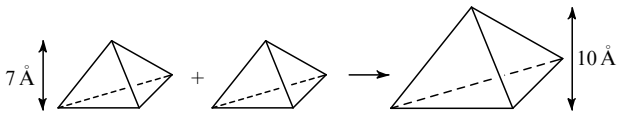
$$TiCl_4 + 2H_2O = TiO_2\downarrow + 4HCl.$$

Unfortunately, most of the colloidal solutions of nanoparticles have low stability towards coagulation and possess a large size dispersion. Coagulation can be prevented by passivation[30] of the surface of nanoparticles by hydroxyl ions,[31] amines,[32] or ammonia.[13] Yet another procedure for the stabilisation of colloidal solutions of nanoparticles is the coating of their surfaces with polyphosphates[33] or thiols.[34–38] As a result, one can obtain a stable colloidal solution of nanoparticles, isolate the nanoparticles as a powder, and then prepare a colloidal solution again by dispersing the powder in a solvent.

Usually, the methods for the synthesis of nanoparticles discussed above result in a nonuniform size distribution. It is possible to decrease the width of this distribution by monitoring the synthetic procedures and using high-pressure liquid chromatography and capillary electrophoresis.[39, 40] In the latter case, the separation of nanoparticles is achieved due to the different charge/size ratios for nanoparticles of different sizes.

Small monodisperse semiconductor clusters can be obtained by performing the synthesis inside zeolite cages.[17–19, 41, 42] Thus Cd_4S_4 clusters were synthesised inside zeolite Y.[17–19]

It is possible to synthesise larger semiconductor nanoparticles of fixed size by introducing additional molecules to a small initial cluster stabilised by organic ligands in a colloidal solution.[7, 43–47] For instance, it was found that the size of CdS clusters coated with thiophenolate ions can be increased if a metal sulfide is added to the solution.[45] Such a polymerisation of inorganic compounds appeared to be applicable to the synthesis of large semiconductor clusters of strictly fixed size from small particles. Wang and Herron[48] succeeded in obtaining the $[Cd_{20}S_{13}(SC_6H_5)_{22}]^{8-}$ clusters containing 55 cadmium and sulfur atoms from the pyramidal $[Cd_{10}S_4(SC_6H_5)_{16}]^{4-}$ clusters containing 30 cadmium and sulfur atoms.[34] The introduction of additional five sulfide ions leads to the fusion of two small clusters into one larger cluster. The process of the formation of a large cluster from two small ones can be illustrated by the following scheme:



The pyramidal structure of the $[Cd_{20}S_{13}(SPh)_{22}]^{8-}$ clusters was confirmed by X-ray analysis. Further addition of sulfide ions made it possible to obtain the $Cd_{32}S_{14}(SC_6H_5)_{36}$ tetrahedral clusters containing 82 cadmium and sulfur atoms.[46]

Usually, it is assumed that the nanoparticles containing several hundreds of atoms have a spherical or ellipsoidal shape. However, recent investigations have shown that the nanoparticles often have clearly defined facets and their shape is analogous to that of macroscopic crystals.[49, 50]

The shape and size of nanoparticles is determined by electron microscopy. For a rough estimation of the size of nanoparticles, it is also possible to use the optical spectra of colloidal solutions. These estimates are based on the dependence of the position of the excitonic band of nanoparticles on their size. However, overestimated values are obtained for small nanoparticles[48] (this problem is discussed in more detail below).

2. Dispersion of macroscopic particles in solutions

It is possible to obtain semiconductor nanoparticles by sonication of colloidal solutions of large particles. Nanoparticles of layered semiconductors are also formed upon mere dissolution of large particles in an appropriate solvent, which was observed for MoS_2 and WS_2.[20] Layered MoS_2-type semiconductors are characterised by a weak van der Waals interaction between separate S–Mo–S layers. In the course of dissolution, the solvent molecules penetrate between the layers of the semiconductor and destroy large particles. In the case of MoS_2, the process of destruction can proceed until the formation of a two-layer particle. No further stratification of the semiconductor occurs, since the formation of single-layer particles is accompanied by a considerable increase in the free energy of the system.[20, 21, 30]

Sonication of a disperse system of large semiconductor particles can also result in the formation of nanoparticles. The nanoparticles of MoS_2, WS_2,[20, 21] PbI_2,[51] and α-Fe_2O_3 [52, 53] were obtained by this procedure.

Nanocrystals of layered PbI_2-type semiconductors have a disk-like shape and discrete 'magic' sizes of the disks.[51] For these semiconductors, a stable nanoparticle of a minimum size is assumed to be the smallest crystallite conserving the hexagonal symmetry of the macroscopic crystal. Such a crystallite is composed of two seven-atom iodine layers and two lead layers. Large stable nanoparticles are obtained from this 'seed' by the layer-by-layer addition of extra iodide 'caps' symmetrically around the perimeter. An analogous structure is also assumed for MoS_2 nanoparticles.[30, 54]

3. Gas-phase synthesis of nanoparticles

The gas-phase synthesis of TiO_2 and Si nanoparticles was carried out by Visca and Matijevic[55] and Fojtik *et al.*[56] Thus the Si nanoparticles are formed in 67% yield in the combustion of SiH_4

under oxygen-deficient conditions as a result of thermolysis of SiH_4.

An interesting method for the gas-phase synthesis of nanoparticles of various materials has been suggested:[23–25] the nanoparticles were obtained by pulsed laser vapourisation of metals in a chamber filled with a known amount of a reagent gas and by controlled condensation of nanoparticles onto the support. A schematic view of the installation for the synthesis of nanoparticles is given in Fig. 1. As the metal atoms diffuse from the target to the support, they interact with the gas to form the desired compound (for instance, oxide in the case of oxygen, nitride for nitrogen or ammonia, carbide for methane, *etc.*).

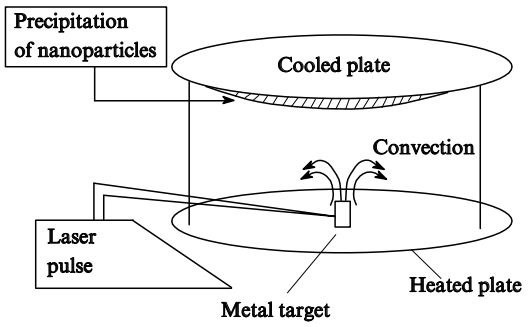


Figure 1. Schematic view of the installation for the synthesis of nanoparticles by laser vapourisation of metals.

The pulsed laser vapourisation of metals in the chamber is a modification of the known method for the synthesis of metal compounds in a diffusion cloud chamber and makes it possible to prepare nanoparticles of mixed molecular composition, such as mixed oxides/nitrides and carbides/nitrides or mixtures of oxides of different metals. Along with the reagent gas, the chamber contains an inert gas, such as He or Ar, at a pressure of 10^{-2}–1 Torr, which favours the establishment of steady convection between the heated bottom plate and cooled top plate. In an experiment with a single pulse of a Nd:YAG laser (532 nm, 15–30 mJ pulse^{-1}, 10^{-8} s), over 10^{14} metal atoms are vapourised. A new compound is formed due to the reaction between the 'hot' metal atoms and the gas molecules, which is accompanied by the energy loss of the molecules formed by collisions with the inert gas atoms. The metal atoms that did not enter into reaction and the molecules of the new compound are carried by convection to the nucleation zone on the cooled top plate. By changing the composition of the inert gas and the reagent gas in the chamber and varying the temperature gradient and laser pulse power, it is possible to control the elemental composition and size of nanoparticles that are obtained.

4. Synthesis of nanoparticles of mixed composition

The high efficiency of recombination of the light-generated electrons and holes presents obstacles to the practical application of the semiconductor nanoparticles in photocatalysis. In this connection, the semiconductor nanocrystal hetero-structures composed of semiconductors with different structures of the electronic levels are of considerable interest. With these structures, it is possible to attain high quantum yields of charge separation. The nanoparticles schematically shown in Fig. 2 belong to this class of hetero-structures. The structures analogous to that shown in Fig. 2 *a* are known for CdS/TiO_2,[57–60] CdS/ZnO,[57,61] CdS/AgI and CdS/HgS,[62,63] Cd_3P_2/TiO_2 and Cd_3P_2/ZnO,[64] and AgI/Ag_2S.[65] For CdS/TiO_2, photoexcitation into the absorption band of CdS results in the electron transfer from CdS to TiO_2, while the hole remains in CdS. These structures are also of interest as nanoscale rectifier units for molecular electronics.[66]

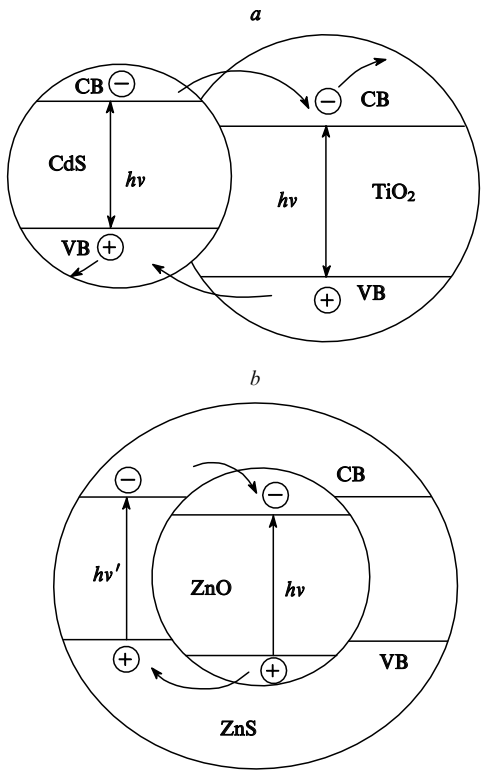


Figure 2. Schematic view of hetero-nanoparticles of different structure. (*a*) and (*b*), see text; CB stands for conduction band; VB stands for valence band.

The formation of hetero-structures of the 'core–shell' type (see Fig. 2 *b*) has been demonstrated using the CdSe/ZnS and ZnS/CdSe nanoparticles as an example.[67] These nanoparticles are obtained by controlled precipitation of semiconductor molecules of one type ('shell') on the pre-synthesised nanoparticles of another type ('core'). The synthesis of the shell is carried out in colloidal solution by methods analogous to those for the synthesis of one-component nanoparticles considered above. The crystalline shells grow on the nanocrystal core despite the fact that the lattice constants in CdSe and in ZnS differ by 13%.

The following 'core-shell' type nanoparticles have also been synthesised: HgS/CdS,[63] ZnS/ZnO and ZnO/ZnSe,[68,69] TiO_2/SiO_2 and TiO_2/SnO_2,[70] and TiO_2/ZnO.[71] These hetero-nanoparticles can, in turn, be coated with a layer of one more semiconductor. Below we shall consider the use of nanocrystal hetero-structures in photocatalysis.

5. Preparation of nanostructured semiconductor films

Thin films of semiconductor nanoparticles are of considerable practical interest. Synthesis of these films is carried out by precipitation of pre-formed nanoparticles from colloidal solutions onto the supports, by direct precipitation of semiconductor molecules onto the support, and by oxidative hydrolysis of the corresponding metal salts at the anode. Usually, the films are 0.1–1 μm thick. The following films of semiconductor nanoparticles are known: SnO_2,[72] ZnO,[61,73] TiO_2,[74] WO_3,[75,76] and Fe_2O_3.[77] The SnO_2, ZnO, TiO_2, and WO_3 films were obtained by precipitation of nanoparticles. Direct precipitation of semiconductor molecules onto the support is used to prepare films of nanoparticles of semiconductors on the basis of Group II–VI elements.

Oxidative hydrolysis of $TiCl_3$ at pH 2.3 and a platinum anode potential of 0 V *vs.* saturated calomel electrode (SCE) results in the formation of nanoparticles with an average diameter of 1–2 nm on the anode surface.[78]

Nanostructured films containing nanoparticles of different semiconductors can be prepared by coprecipitation. A schematic view of such a film supported by the optically transparent electrode is given in Fig. 3. Yet another method for the preparation of such films consists in wetting of a plate coated with a film of a certain type of nanoparticles with a solution containing metal ions followed by wetting of the plate with a solution containing sulfide ions. This procedure was used for the synthesis of films containing ZnO and CdS nanoparticles.[61, 79]

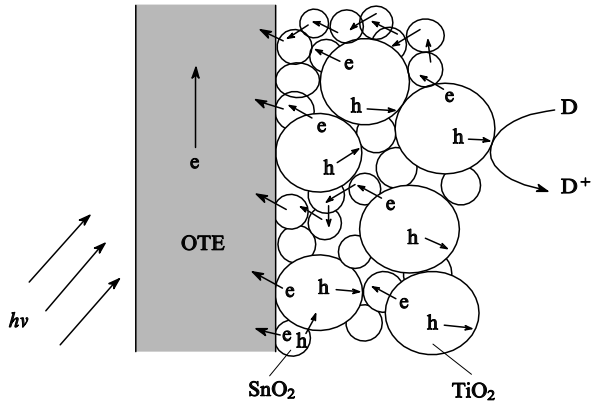


Figure 3. Schematic view of the process of photostimulated charge separation in the nanostructured film composed of TiO_2 and SnO_2 nanoparticles adsorbed on an optically transparent electrode (OTE).

III. The quantum size effects

1. Specific features of the kinetics of chemical processes on the surface of nanoparticles

Surface reactions determine the behaviour of nanoparticles in colloidal solutions and the possibility of using the semiconductor nanoparticles in photocatalysis. For reagents adsorbed on the surface of nanoparticles, a chemical reaction cannot be considered as a process occurring in an infinite volume with a constant average density of the molecules. This is associated with the fact that the surface area of nanoparticles is rather small and comparable with the size of the reagents. In such a system, the kinetics of a bimolecular chemical reaction differs from the classical kinetics.

The mathematical approach to the classical, or deterministic, chemical kinetics ignores fluctuations in the concentration of reacting molecules. However, the nanoparticles composed of a small number of reacting molecules are characterised by relatively large fluctuations in the number of reagents. This results in different changes in the concentration of reagents on the surface of different nanoparticles with time; the general kinetic law for a macroscopic sample can be obtained by averaging the kinetics over all nanoparticles. A mathematical description of the processes occurring in such systems is based on the use of a stochastic approach, which takes into account the statistical fluctuations in the number of reacting molecules.[80]

General regularities in the kinetics of diffusion-controlled reactions for a small number of reacting molecules have been analysed.[81, 82] The kinetics of a bimolecular reaction was analysed assuming that the reaction can be characterised by the rate constant k, which is the same for all the reagent pairs. The results of these studies can be used for the analysis of the kinetics of reactions occurring on the surface of nanoparticles.

For a reaction

$$A + A \xrightarrow{k} C \qquad (2)$$

the kinetics of the loss of the reagents is described by the following equation:[83]

$$\frac{\bar{N}(t)}{\bar{N}(0)} = \sum_{n=1}^{\infty} B_n \exp\left[-\frac{1}{2}n(n-1)kt\right] \qquad (3)$$

where $\bar{N}(t)$ and $\bar{N}(0)$ are the current and initial concentrations of the reagents on the surface of nanoparticles averaged over the sample containing a macroscopic number of nanoparticles,

$$B_n = \frac{(2n-1)}{2^n}\,\frac{\exp[-\bar{N}(0)]}{\bar{N}(0)}\sum_{j=n}^{\infty}\frac{\bar{N}(0)^j}{(j-n)!}\,\frac{\Gamma[(j-n+1)/2]}{\Gamma[(j+n+1)/2]},$$

$j = n, n+2, n+4, \ldots$

and $\Gamma(x)$ is the gamma function.

The assumption in Eqn (3) that the rate constant k is the same for all the reagent pairs may appear to be invalid for small nanoparticles. Actually, it was shown[84] that Eqn (3) is only valid for nanoparticles the size of which exceeds that of the reagents by at least an order of magnitude. In Fig. 4, the results of the analysis of the kinetic curves of the reaction occurring on the surface within a circle of radius R are presented as an example. The analysis was performed using Eqn (3) and the curves were calculated by the Monte Carlo method for various size of the reagent particles and the circle. The triplet – triplet annihilation of molecules recombining at a distance of R_{ef} was considered as a model reaction. It can be seen that for $R < 10R_{ef}$ the k value becomes dependent on the radius of the circle and, hence, Eqn (3) is no longer valid for small radii R.

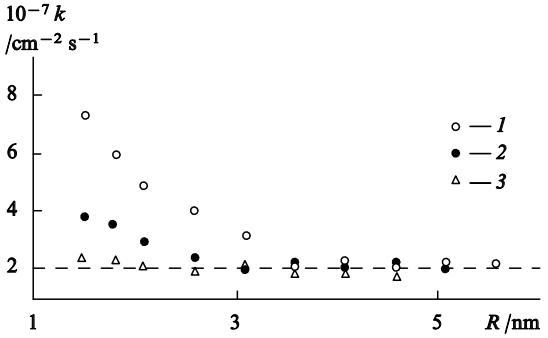


Figure 4. The dependence of the rate constant for the triplet – triplet annihilation on the circle radius for different effective radii of the triplet – triplet annihilation.
R_{ef} /Å: (*1*) 4.3; (*2*) 2.9; (*3*) 2.3.

The Monte Carlo method can also be used for the description of the kinetics of processes on the surface of nanoparticles. The number of reagent molecules on the surface of each nanoparticle is small, and calculations of the reaction kinetics by the Monte Carlo method do not require much effort. The parameters of the process used in the calculations are chosen so as to achieve the best agreement between the calculated and experimental kinetic dependences.[84, 85]

Only a few processes occurring on the surface of nanoparticles have been studied to date. The triplet – triplet annihilation of the zinc tetraphenylporphyrin (ZnTPP) molecules adsorbed on the surface of disk-like MoS_2 nanoparticles, whose size did not exceed 2 nm, has been studied.[86] The annihilation of the triplet molecules occurs by an exchange mechanism and its efficiency (w) is determined by the distance between the reagents (r)[87, 88]

$$w(r) = v\exp\left(\frac{-2r}{a}\right), \qquad (4)$$

where v and a are the parameters of the process.

Typical curves of decay of triplet-excited molecules on the surface of MoS_2 nanoparticles and the results of their analysis by the Monte Carlo method are shown in Fig. 5. This analysis appeared to be very 'sensitive' to the parameters of the interaction

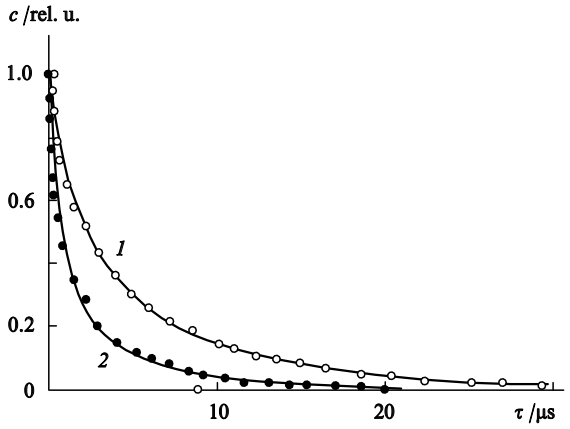


Figure 5. The decay curves of triplet-excited ZnTPP molecules on the surface of the MoS_2 nanoparticles.
The average number of the triplet-excited ZnTPP molecules on the surface of the MoS_2 nanoparticles is equal to 6.4 (*1*) and 22 (*2*); the lines correspond to the experimental data, the dots correspond to the results of the Monte Carlo calculations.

between the triplet molecules and their diffusion over the surface of MoS_2 nanoparticles. The following values of the parameters were obtained: $v = 10^6\ s^{-1}$ and $a = 3$ Å, and the diffusion coefficient of the zinc porphyrin molecules over the surface (D) was found to be equal to $10^{-8}\ cm^2\ s^{-1}$.

Quenching of the singly excited molecules of ZnTPP and its metal-free analogue (H_2TPP) by various quinones (Q) on the surface of the MoS_2 nanoparticles has been studied.[84] The kinetics of the processes was analysed by both the Monte Carlo method and kinetic equations[85] derived for the reactions occurring on the surface of the disk-like nanoparticles. The decay curves of the singlet-excited H_2TPP molecules in the reaction with duroquinone (DQ)

$$H_2TPP^* + DQ \longrightarrow H_2TPP^+ + DQ^- \qquad (5)$$

are shown as an example in Fig. 6.

The theoretical decay curves (dots in Fig. 6) calculated by the Monte Carlo method are in good agreement with the experimental ones.

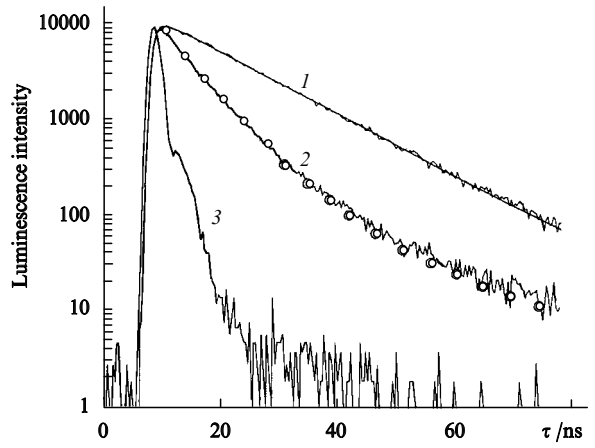


Figure 6. The kinetics of the luminescence decay of the singlet-excited H_2TPP molecules on the surface of the MoS_2 nanoparticles;
(*1*) in the absence of the quencher; (*2*) each nanoparticle is capped, on the average, with five duroquinone molecules; (*3*) the shape of the excitation light pulse. The dots on curve *2* correspond to the results of the Monte Carlo calculations.[84]

The detailed kinetic analysis of bimolecular processes of electron and energy transfer on the surface of nanoparticles of various shapes has been carried out.[84,89] It has been possible to obtain an analytical solution of the kinetic problem only for the reactions occurring on the surface of planar disk-like nanoparticles. It has been shown that the corresponding equations derived for the disk-like nanoparticles can be applied to nanoparticles of different (*viz.*, cubic, spherical, and tetrahedral) shape.

The kinetic equations for the processes of electron and energy transfer on the surface of nanoparticles are rather complicated. For example, the kinetics of electron transfer from a donor to acceptors on the surface of disk-like nanoparticles is described by the following equation:[85]

$$\frac{N(t)}{N(0)} = \qquad (6)$$

$$= \frac{2}{R^2}\int_0^R r_0 \exp\left\{-\bar{n}\left[1 - \exp\left\{-\frac{1}{\pi(R^2 - d^2)}\mathrm{f}(r_0, t)\right\}\right]\right\}\mathrm{d}r_0 ,$$

where $\bar{n}$ is the average number of the acceptor molecules on each surface of a disk-like nanoparticle, d is the sum of the donor and acceptor radii,

$$\mathrm{f}(r_0,t) = \int_d^{R+r_0} \left\{1 - \exp[-w(r)t]\right\} 2r\varphi_{\max}\mathrm{d}r , \qquad (6a)$$

$w(r)$ is the function describing the dependence of the probability of the electron transfer from the donor to the acceptor on the distance between them, and the meaning of other parameters is evident from Fig. 7.

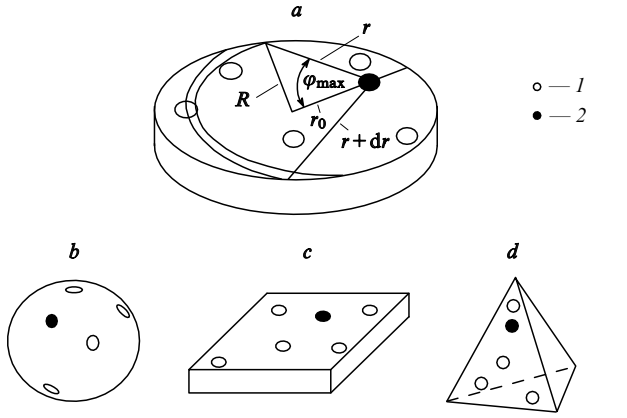


Figure 7. Disk-like (*a*), spherical (*b*), square (*c*), and pyramidal (*d*) nanoparticles.
The acceptor (*1*) and donor (*2*) species.

The use of the kinetic equations similar to Eqn (6) for the description of the processes on the surface of nanoparticles requires time-consuming calculations. In this connection, the problem of applicability of simpler kinetic equations derived for the processes occurring on the unbounded surface to nanoparticles appears to be important.[89]

To solve this problem, an analysis according to the following scheme was performed in considering specific equations used for the description of the processes occurring with participation of nanoparticles. First, the decay curves of the reagents on the surface of nanoparticles were calculated by the Monte Carlo method. Then, these curves were considered as 'experimental' kinetic curves and were used to find the characteristics of the process using the corresponding kinetic equations. The coincidence between the calculated characteristics and the

corresponding parameters used in the calculations of the kinetic curves by the Monte Carlo method served as the criterion of the applicability of the kinetic equations for the description of the processes occurring on the surface of nanoparticles.

It was shown[84, 89] that the classical equations of chemical kinetics can be used to determine the parameters of the processes occurring on the surface of nanoparticles down to their characteristic linear size that is 2–7 times larger than the size of reacting molecules or effective radii of the interaction between them. The application of the classical equations of chemical kinetics to nanoparticles of smaller size results in considerable errors in the calculations of characteristics of the processes. For small nanoparticles, the parameters of chemical reactions can be calculated using the corresponding equations for the nanoparticles or by the Monte Carlo method.

The following equation is an analogue of Eqn (6) for an unbounded surface and the $w(r)$ function defined by Eqn (4):

$$\frac{N(t)}{N(0)} = \exp\left[-c\left(\frac{\pi a^2}{4}\ln^2 \nu t - \pi d^2\right)\right], \tag{7}$$

where c is the surface concentration of an acceptor. The possibility of using Eqn (7) to analyse the kinetic curves on the surface of disk-like nanoparticles of various size has been considered.[89] It was shown that Eqn (7) can be used for calculating the parameters of interaction between the reagents (a and ν) down to the disk size 7 times greater than the sum of the donor and acceptor radii.

2. The effect of the nanoparticle size on their optical and luminescent characteristics

a. Dependence of the optical and luminescent characteristics of nanoparticles on their size

It seems evident that the excitation energy of small semiconductor crystals must differ from that of a large semiconductor. In fact, the energy of the electronic excitation of an isolated molecule is usually considerably higher than the energy of the interband transition in the corresponding macroscopic semiconductor. Hence, a size range must exist in which the low energy of the electronic excitation of a crystal changes smoothly to the high value characterising the individual molecule on going from the crystal to the molecule. For semiconductor crystals, such a transition occurs in the nanometric range. So far, the effect of the nanoparticle size on their optical spectra has been found for many types of semiconductors.[3, 38, 90–108] The optical spectra of CdSe nanoparticles of various size are shown in Fig. 8 *a* as an example.[108] It can be seen that the absorption band of nanoparticles does shift to the shorter wavelength (blue) region as their size decreases.

The quantitative dependence of the minimum electronic excitation energy of a nanoparticle on its size can be approximately calculated taking into account the relation between the uncertainty in the position (Δx) and the uncertainty in the momentum (Δp) of the exciton in a macroscopic crystal and in a nanoparticle:

$$\Delta p \Delta x \geqslant \frac{\hbar}{2}. \tag{8}$$

The delocalised exciton has no fixed position in the periodic potential of the macroscopic crystal, whereas its energy (E) and momentum ($p = \hbar k$) are strictly fixed, and at small k

$$E = \frac{\hbar^2 k^2}{2\mu}, \tag{9}$$

where μ is the effective mass of the exciton.[109] For a nanoparticle, the uncertainty in the position of the exciton depends on the characteristic size of the nanoparticle

$$\Delta x = d.$$

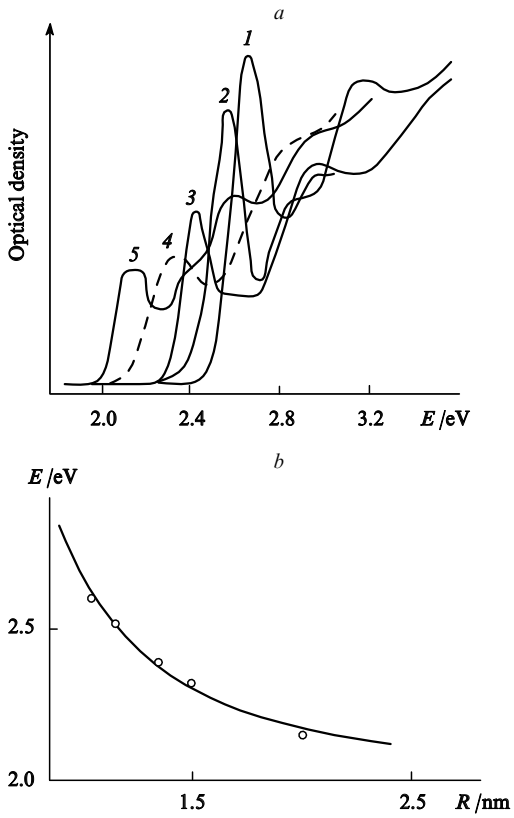


Figure 8. The absorption spectra of the CdSe nanoparticles of various size (*a*) and the dependence of the energy at the maximum of the absorption band of the CdSe nanoparticles on their radius (*b*).
(*a*): R /nm: (*1*) 2.1; (*2*) 2.3; (*3*) 2.7; (*4*) 3; (*5*) 4; (*b*) the line corresponds to the $1/R^2$ dependence.

Assuming that the relation between the energy and momentum is independent of the particle size, the exciton energy will change in inverse proportion to the square of the characteristic size of the nanoparticle.

A more rigorous analysis of the effect of the size on the energy of excitonic excitation of spherical nanoparticles (E_n) gives the following relationship:

$$E_n = E_m + E_l, \tag{10}$$

where E_m is the energy of the interband transition in a macroscopic semiconductor, E_l is the energy of exciton localisation in the nanoparticle:

$$E_l = \frac{h^2 n^2}{8R^2\mu} - \frac{1.78e^2}{\varepsilon R} - 0.248E_R^*, \tag{11}$$

where n is an integer, R is the radius of the nanoparticle, $\mu = (m_e^{-1} + m_h^{-1})^{-1}$ (m_e and m_h are the electron and hole effective mass, respectively), ε is the dielectric constant of the semiconductor, and E_R^* is the effective Rydberg energy.[1, 2, 110] The first term on the right of the equation is predominant, and its nature was considered above, the second term takes into account the Coulomb interaction between the electron and hole inside the nanoparticle, and the third term is responsible for the spatial correlation. The n values larger than 1 in Eqn (11) correspond to the exciton transitions to higher excited states (see Fig. 8 *a*).

In the case of anisotropic semiconductors, the electron and hole effective masses depend on the direction of motion and Eqn (11) becomes more complex with allowance for this anisotropy [51]

$$E_{n_x,n_y,n_z} = \frac{h^2}{8}\left(\frac{n_x^2}{\mu_x L_x^2} + \frac{n_y^2}{\mu_y L_y^2} + \frac{n_z^2}{\mu_z L_z^2}\right) - \frac{1.78e^2}{\varepsilon R} - 0.243E_R^*\,, \quad (12)$$

where n_x, n_y, and n_z are integers; μ_x, μ_y, and μ_z are the effective masses of the exciton along the corresponding directions, and L_x, L_y, and L_z are the dimensions of the nanoparticle.

The dependence of the energy at the maximum of the absorption band of CdSe nanoparticles on their radii calculated from the data in Fig. 8 *a* is shown in Fig. 8 *b*. It can be seen that the exciton energy of nanoparticles is well described by the $1/R^2$ dependence.

The effective mass approximation and, hence, Eqn (11) become inapplicable for small nanoparticles. The observed values of the exciton energies of nanoparticles appear to be lower than those predicted from Eqn (11). A more exact expression for the exciton energy can be found by quantum-chemical methods.[111, 112] However, quantum-chemical calculations cannot also be applied to very small nanoparticles. The lower confidence level of the exciton energy calculations varies for different semiconductors. In the case of the effective mass approximation, it is determined by the value of the Bohr radius of the exciton. The dependence of the energy of the first excitonic CdS band on the nanoparticle size and the results of the corresponding calculations performed in the effective mass approximation[48] and by quantum-chemical methods[113] are shown in Fig. 9 as an example.

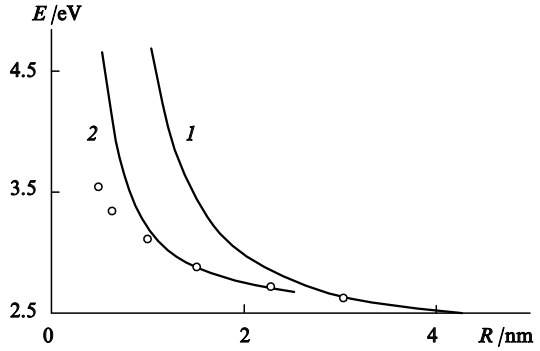


Figure 9. Dependence of the energy of the first excitonic band of CdS on the nanoparticle size and the results of the corresponding calculations performed in the effective mass approximation (*1*)[48] and by quantum-chemical methods (*2*).[113]

Equation (11) is often used for the estimation of the size of nanoparticles. Usually, the last two terms on the right side of this equation are neglected. For the first excitonic transition we have

$$R = \frac{h}{\sqrt{8\mu E_1}}\,. \quad (13)$$

As was mentioned above, the effective mass approximation and, hence, Eqn (13) is inapplicable for very small nanoparticles. The use of Eqn (13) results in overestimation of the size of nanoparticles; the smaller the true size of nanoparticles the larger the overestimation.

Another manifestation of the size effect in the optical characteristics of nanoparticles is the blue shift of their optical spectrum, which occurs when an excess electron is injected into the nanoparticle.[114–121] Three different reasons may account for the shift: first, the increase in the exciton energy due to the influence of the electric field of the excess electron;[119, 121] second, the effect of filling the lowest vacant state with the excess electron whose excitation to a higher vacant state requires higher energy;[122, 123] and third, a decrease in the oscillator strength of the excitonic transition due to the effect of trapped electrons and holes.[13, 124]

Recombination of light-generated charges results in luminescence of nanoparticles. In this case, the blue shift is also observed as the nanoparticle size decreases. The luminescence of ZnO,[61, 68, 68, 117] ZnS,[125–127] CdS,[128–136] and CdSe[137, 138] has been studied in detail.

The luminescence spectra of colloidal CdS solutions are shown in Fig. 10. It can be seen that the decrease in the nanoparticle size results in a shift of the luminescence spectra towards the short-wavelength region. The kinetics of the luminescence decay of nanoparticles is nonexponential and the characteristic time of decay for nanoparticles of the same size depends on the luminescence wavelength. The shorter-lived luminescence corresponds to a higher energy of the emitted light quantum. The dependence of the lifetime of the excited state on the wavelength is explained by the contribution of the Coulomb interaction between the electron and hole to the energy of the emitted light quantum:[139]

$$h\nu = E - (D_+ - D_-) + \frac{e^2}{\varepsilon R_h}\,, \quad (14)$$

where E is the minimum excitation energy of nanoparticles, D_- and D_+ are the depths of the electron and hole traps, respectively, and R_h is the distance between the electron and hole. If the electron–hole recombination follows the tunnel mechanism, then the pairs with small R_h emit light faster and at higher energies than the pairs with larger R_h.

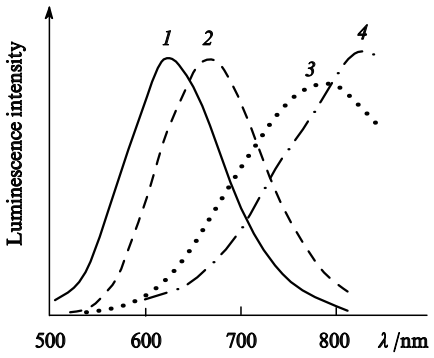


Figure 10. The luminescence spectra of colloidal solutions of CdS nanoparticles in acetonitrile.[131]
Average size of nanoparticles /nm: (*1*) 2.5; (*2*) 3; (*3*) 3.7; (*4*) >4.2.

b. Dependence of the intensity of electronic transitions and radiative lifetimes on the nanoparticle size.

The increase in the volume-normalised oscillator strength of the excitonic absorption with the decrease in the size of nanoparticles[110, 140–143] is one more manifestation of the quantum size effect. This is associated with the increase in the overlap integral of the electron and hole wave functions with the decrease in the size of nanoparticles.

For large spherical semiconductor particles ($R \gg a_B$, where a_B is the Bohr radius), the overlap integral of the wave functions is independent of the particle size and the oscillator strength of excitonic absorption (f) is determined by the macroscopic dipole moment of the transition. Assuming that the exciton moves coherently throughout the particle, the number of energy levels in the excitonic band is equal to $(R/a_B)^3$ (see Ref. 110). In the low-temperature limit, the integrated oscillator strength of all $(R/a_B)^3$ levels is concentrated in the lowest excitonic transition. The oscillator strength of the particle increases linearly as the volume increases

$$f \propto \left(\frac{R}{a_B}\right)^3,$$

whereas the volume-normalised oscillator strength (f/V) remains unchanged.

For nanoparticles ($R \leqslant a_B$), the overlap integral of the electron and hole wave functions increases as the nanoparticle size decreases. As a result, the oscillator strength of nanoparticles depends only slightly on their size, while the volume-normalised oscillator strength increases with decrease in the nanoparticle size

$$\frac{f}{V} \propto \left(\frac{a_B}{R}\right)^3 .$$

As is known, the oscillator strength determines the radiative lifetime of excited state at low temperatures, while the volume-normalised oscillator strength determines the light absorption coefficient. It follows from the analysis performed above that the radiative lifetime of the exciton decreases while the absorption coefficient increases linearly as the nanoparticle volume increases. For typical semiconductor crystals, the excitonic band width is of the order of 0.15–0.3 eV. The possibility for the integrated oscillator strength to be concentrated on the transitions whose widths are of the order of 10^{-3}–10^{-4} eV with the decrease in the nanoparticle size results in a giant increase in the excitonic absorption of nanocrystals. These effects have been observed experimentally.[2, 13, 108, 143] However, complete quantitative agreement between the experimental data and the theoretical concepts of the light absorption by nanoparticles cannot be achieved because of the difficulties in obtaining nanoparticles of fixed size and the effect of surface defects on the processes of light absorption and emission by nanoparticles.

3. Redox properties of semiconductor nanoparticles

Evidently, changes in the nanoparticle size resulting in the change in the energy of formation of electron–hole centres affect the redox properties of light-irradiated semiconductor nanocrystals. It seems most likely that the conduction and valence bands may be shifted towards more negative and more positive potentials, respectively, by decreasing the size of semiconductor nanoparticles. The energy diagram for CdTe nanocrystals [144] is shown in Fig. 11 as an example. It can be seen that the decrease in the size of nanoparticles affects more strongly the position of the energy level of the electron centre than that of the hole centre.

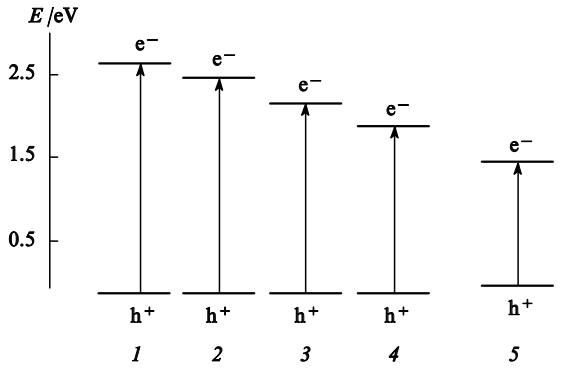


Figure 11. The energy diagram of the CdTe nanoparticles. Average size of the nanoparticles /nm: (*1*) 1; (*2*) 1.25; (*3*) 1.75; (*4*) 2; (*5*) ∞ (the last corresponds to the macroscopic crystal).

According to the modern theoretical concepts of the electron transfer,[87, 145, 146] an appreciable change in the position of the energy level of the electron centre may result in a considerable change in the rate of redox processes occurring with the participation of nanoparticles. The dependence of the rate constant for the luminescence quenching of light-irradiated MoS_2 nanoparticles by oxygen molecules on the particle size [30, 54] is shown in Fig. 12. The processes occurring in the MoS_2 nanoparticles upon their irradiation by light are described by the following scheme:

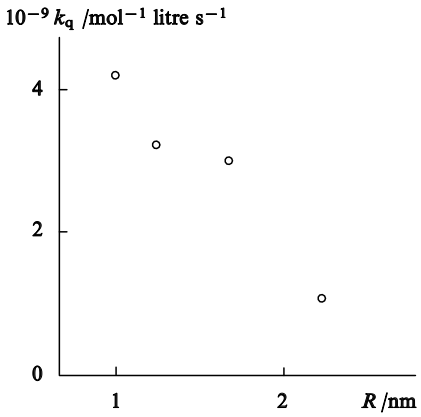


Figure 12. Dependence of the rate constant for the oxygen quenching of the luminescence of light-irradiated MoS_2 nanoparticles on their size.

Photogeneration of charge carriers:

$$MoS_2 \xrightarrow{h\nu} MoS_2(e^- \ldots h^+); \quad (15)$$

stabilisation of charge carriers in shallow traps:

$$e^- + ST \longrightarrow e_t^- , \quad (16)$$

$$h^+ + ST \longrightarrow h_t^+ ; \quad (17)$$

recombination luminescence:

$$e_t^- + h_t^+ \longrightarrow h\nu ; \quad (18)$$

luminescence quenching:

$$e_t^- + O_2 \longrightarrow \text{quenching}. \quad (19)$$

The luminescence of MoS_2 nanoparticles is due to the recombination of electrons trapped into shallow traps (e_t^-) and holes (h_t^+). In the presence of oxygen, luminescence quenching is observed due to the electron transfer from the trap to O_2. A decrease in the size of MoS_2 nanoparticles results in an increase in the energy of the trapped electrons and, hence, in an increase in thermal effect of the process. According to the modern concepts of electron transfer in the condensed phase,[87, 145–147] the reaction rate of the electron transfer from the trap to the oxygen molecule must also increase in this case.

It is of note that the potential of the bottom of the conduction band of the macroscopic MoS_2 semiconductor is equal to 0.2 V *vs.* SCE, while the reduction potential of the oxygen molecule is equal to 0.82 V *vs.* SCE.[148] Comparison of these values shows that the photoreduction of oxygen using a macroscopic MoS_2 crystal is thermodynamically impossible.

The dependences analogous to that shown in Fig. 12 were found for the luminescence quenching of MoS_2 nanoparticles by methyl viologen and nitrobenzene.[30, 54]

A dependence of the quenching efficiency of singlet-excited ZnTPP molecules by CdS nanoparticles on the nanoparticle size was found by Chrysochoos.[149] Analysis of experimental data[149] has shown[84] that the rate constant for quenching (k_q) changes from 0 to 10^{12} mol litre^{-1} s^{-1} as the localisation energy of the exciton in the CdS nanoparticles changes from 0.7 to 0.5 eV. From the results shown in Fig. 9 one can easily estimate that the change in the nanoparticle size from $\sim$0.8 to $\sim$1.2 nm corresponds to this range of the change in the localisation energy of the exciton. Large values of the quenching rate constant ($\sim 10^{12}$ mol litre^{-1} s^{-1}) indicate that it was quenching of the porphyrin molecules adsorbed on the surface of CdS nanoparticles that has been observed by Chrysochoos.[149]

4. Dependence of thermodynamic parameters of nanocrystals on their size

As has been mentioned above, a considerable portion of the atoms of nanoparticles is on the surface and it increases as the nanoparticle size decreases. Correspondingly, the surface atoms make a large contribution to the nanocrystal energy. In this connection, the dependence of the melting temperature of nanoparticles on their size shown in Fig. 13 for CdS[150] becomes understandable. In fact, the surface energy of a liquid is always lower than the surface energy of the corresponding crystal. A decrease in the size of nanoparticles leads to an increase in the proportion of the surface energy and, hence, to a decrease in the melting temperature of nanocrystals. As can be seen from Fig. 13, this decrease can be considerable.

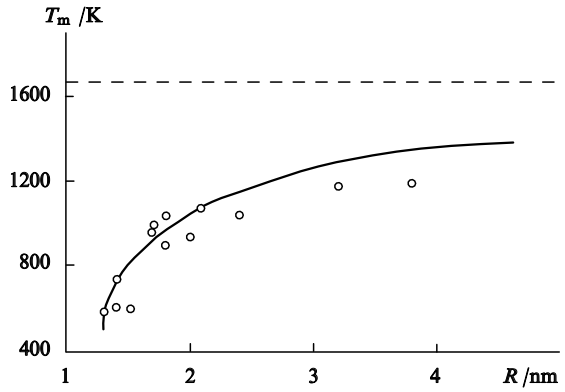


Figure 13. Dependence of the melting temperature (T_m) of CdS nanoparticles on their size.[150]

The geometry of the crystal lattice of a macroscopic crystal can be changed by applying hydrostatic pressure to the crystal, whch results in closer crystal packing. An analogous transformation can also be performed for nanocrystals. Thus, the application of hydrostatic pressure to the CdSe nanocrystal with the wurtzite type structure (hexagonal crystal lattice) results in the change to the sphalerite type structure (face-centred cubic crystal lattice). As a result, a less ordered surface with high surface energy is formed. Therefore, one should expect that increased pressure (P) is necessary for changing the crystal lattice geometry as the nanocrystal size decreases because of the large fraction of surface centres characteristic of nanocrystals. These are just the dependences of P on the nanoparticle size that were found for CdSe,[151] CdS,[152] InP, and Si.[153] However, in the case of colloidal solutions of nanoparticles it could be expected that both the magnitude and sign of the effect must be strongly dependent on the nature of the solvent molecules coordinated on the surface of nanoparticles and thus affecting the surface energetics in both structural modifications of nanocrystals. The dependence of P on the size of CdSe nanoparticles[151] is shown in Fig. 14 as an example.

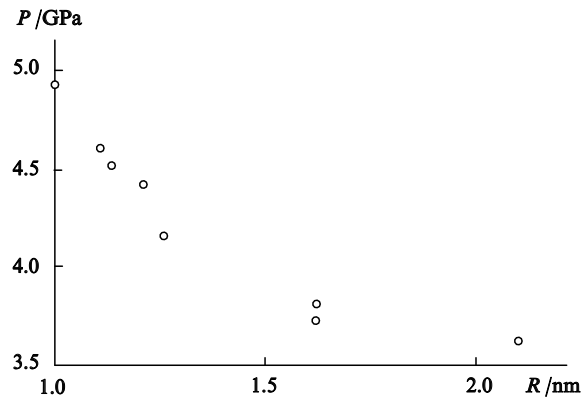


Figure 14. Dependence of hydrostatic pressure necessary for the phase transition to occur on the size of the CdSe nanoparticles.[150]

IV. Photocatalytic processes with the participation of semiconductor nanostructures

Unusual physicochemical properties of semiconductor nanoparticles gave rise to various speculations concerning their practical implementations. Sensors and systems of light energy storage, electronics and photodetoxication of waste waters, non-linear optics and catalysis, and lithography and lasers (see, for example, Refs 154 and 155) are considered as possible fields of uses of semiconductor nanoparticles. However, in most cases it is premature to discuss practical application of semiconductor nanoparticles. Only investigations in the field of photocatalysis carried out so far make it possible to consider the possibilities of practical use of nanoparticles.

1. The use of semiconductor nanoparticles in photocatalytic processes

As has been mentioned above, a decrease in the size of semiconductor nanoparticles results in a shift of the conduction and valence bands towards more negative and more positive potentials, respectively. It seems to be tempting to use the possibility of controlling the redox properties of nanoparticles by changing their size in photocatalytic systems of water decomposition and the synthesis and destruction of organic compounds. Additionally, the fact that nanoparticles have a large specific surface area is of importance for carrying out photocatalytic processes on the surface of semiconductors. And finally, the small size of semiconductor nanoparticles can provide high efficiency of detrapping of light-generated electrons and holes, thus increasing the probability of a photocatalytic process on the surface of the semiconductor.

However, it should be noted that the semiconductor nanoparticles used in photocatalytic studies are, as a rule, rather large ($\sim 10^2$ nm) and no pronounced quantum size effects are observed for them. A correlation between the photocatalytic activity of TiO_2 nanoparticles and their size was found only in one study.[156] High quantum efficiencies of photocatalytic processes with the participation of nanoparticles are achieved by designing specifically ordered structures based on these particles.

The idea of using nanoparticles for photocatalytic water decomposition was first proposed by Henglein[157] and Duonghong *et al.*,[158] who have demonstrated the possibility of photoreduction of methyl viologen in colloidal solutions of semiconductors. The photoreduction of methyl viologen on the surface of nanoparticles was studied by laser flash photolysis in colloidal solutions of TiO_2 [158–166] and metal chalcogenides.[65, 167–170] Photoreduction of various dyes by nanoparticles has also been studied.[171–175] Photoexcitation of nanoparticles results in one-electron reduction of dye molecules followed by the formation of a leuco-product.

The possibility of using nanoparticles in photocatalytic synthesis of organic compounds was demonstrated for the first time by Kraeutler *et al.*[176–178] Photocatalytic synthesis of an amino acid and the Kolbe reaction were carried out by the interband excitation of TiO_2 nanoparticles coated with platinum. Later, *cis–trans* isomerisation of styrene derivatives upon photoexcitation of CdS nanoparticles was reported.[179, 180] The process of isomerisation includes the formation of alkene radical cation on the surface of nanoparticles. Photocatalytic processes of oxidation of a number of alkanes, arenes, amines, and alcohols on the surface of nanoparticles are also known.[181, 182]

Light-generated holes can be used in photooxidation of various substrates on the surface of nanoparticles until their complete destruction.[131, 160, 168, 172, 183–188] The use of semicon-

ductor nanoparticles for photochemical purification of water from various contaminants seems to be rather tempting and attracts particular interest of researchers in recent years. Systems based on TiO_2 seem to be the most promising for photocatalytic mineralisation of organic compounds in waste waters.

Of the three major structural modifications of TiO_2 (rutile, anatase, and brookite), anatase is the most photocatalytically active. The difference in the photocatalytic activity of different TiO_2 modifications is most likely due to their different crystal structures. Anatase has a bandgap of 3.2 eV and UV radiation needs to be applied for the electronic excitation of this compound; hence, only a small portion of the sun light can be used for the photocatalytic processes involving anatase to occur. Nevertheless, among a wide variety of semiconductor materials, TiO_2 is most often used as a photocatalyst due to the high oxidation ability of its photogenerated holes ($E = 2.9$ V *vs.* NHE at pH 0), its stability in aqueous solutions, safety for living organisms, and low price.

Titanium dioxide has long been used in paint industry as the photocatalyst in the oxidation of organic substances. This property of TiO_2 has determined its wide use as the white pigment.[189] Later, attempts were made aimed at using TiO_2 for photodecomposition of water.[190, 191] However, its efficiency appeared to be low because of a low quantum yield of charge photoseparation. Recently, the problems of the environment protection forced many researchers to direct their attention again to the systems based on TiO_2 and to make efforts to use TiO_2 for photocatalytic mineralisation of ecologically hazardous organic compounds both in aqueous media and gases.

The scheme of the photocatalytic process involving semiconductor nanoparticles is shown in Fig. 15. The absorption of a light quantum with an energy of $h\nu$, that exceeds the bandgap of the semiconductor, results in the primary charge separation. In this case, the nanoparticle can be considered as a short-circuit electrode initiating the processes of oxidation and reduction of the substrate molecules adsorbed on the surface. The oxidation and reduction of non-adsorbed substrate molecules is possible if the primary electrons and holes are transformed into stable intermediates on the surface of nanoparticles.

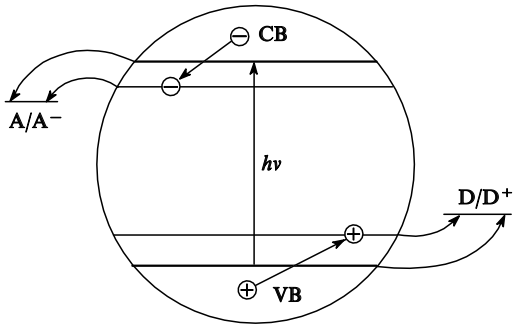


Figure 15. Schematic view of charge separation processes in a semiconductor nanoparticle.

Good results have been obtained for the detoxication of waste waters containing hydrocarbons, phenols, chloroaromatic compounds, surfactants, and nitro compounds (see, for example, reviews[192–196] and references cited therein). A typical example of photocatalytic mineralisation is the oxidation of the dichloroacetate ion by oxygen in water:

$$CHCl_2COO^- + O_2 \xrightarrow{h\nu,\ TiO_2} 2CO_2 + H^+ + Cl_2^- . \qquad (20)$$

The detailed mechanism of the processes of the photoreduction of acceptors and photooxidation of donors with the participation of TiO_2 nanoparticles includes a large number of events occurring both in the bulk and on the surface of nanoparticles; the basic events are outlined below (see also Fig. 16):[196]

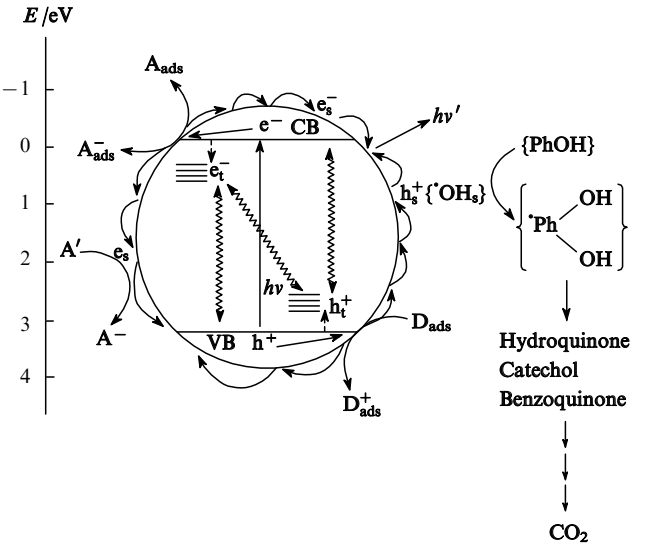


Figure 16. Schematic view of processes of photoreduction of acceptors and photooxidation of donors by TiO_2 nanoparticles.

Photostimulated generation of electrons and holes in the conduction and valence band, respectively

$$TiO_2 \xrightarrow{h\nu} TiO_2(e^- + h^+) ; \qquad (21)$$

charge carrier migration to the surface of the nanoparticle

$$e^- \longrightarrow e_s^- , \qquad (22)$$

$$h^+ \longrightarrow h_s^+ , \qquad (23)$$

$$(e_s^-, h_s^+) \longrightarrow \text{surface migration;} \qquad (24)$$

charge carrier trapping by acceptor centres and into shallow traps (ST)

$$e^- + (ST)_e \longrightarrow e_t^- , \qquad (25)$$

$$h^+ + (ST)_h \longrightarrow h_t^+ , \qquad (26)$$

$$e_s^- + A_s \longrightarrow A_s^- , \qquad (27)$$

$$h_s^+ + D_s \longrightarrow D_s^+ , \qquad (28)$$

$$e^- + Ti^{IV} \longrightarrow Ti^{3+} , \qquad (29)$$

$$h^+ + Ti^{IV}-OH^- \longrightarrow Ti^{IV}-OH^\bullet , \qquad (30)$$

$$e^- + O_2\,(\text{surface}) \longrightarrow O_2^{-\bullet}\,(\text{surface}); \qquad (31)$$

charge carrier recombination (radiative and nonradiative)

$$e^-, e_t^- + h^+, h_t^+ \longrightarrow h\nu , \qquad (32)$$

$$Ti^{IV}-OH^\bullet + Ti^{3+} \longrightarrow h\nu + 2Ti^{IV} , \qquad (33)$$

$$Ti^{IV}-OH^\bullet + Ti^{3+} + O_2^{-\bullet}\,(\text{surface}) \longrightarrow h\nu + 2Ti^{IV} . \qquad (34)$$

It is usually assumed that the photooxidation of organic substrates in aqueous suspensions of TiO_2 can occur by both the direct interaction of the holes with the substrate molecules and the formation of the $OH\cdot$ radicals in the reaction of the holes with H_2O or OH^-.

The prospects of the use of semiconductor nanoparticles in photocatalysis have stimulated studies of the possibility of spectral sensitisation of nanoparticles and modification of their surface by noble metals. In the photocatalytic systems of water decomposition, the metal deposited on the surface of nanoparticles acts as the catalyst of the photosplitting of water to produce hydrogen gas. The effect of coating the surface of TiO_2 nanoparticles with platinum[197, 198] and other noble metals and metal oxides[199–202] on the quantum yield of water photodegradation has been studied.

Sensitisation of semiconductors is widely used for expanding the spectral sensitivity region of these materials. Thus, TiO_2 has a bandgap of 3.1 eV and its use in a photocatalytic system is only expedient in the case of expanding the spectral sensitivity region of the system into the visible region. Sensitisation of TiO_2 nanoparticles is performed with the participation of both singlet [203–206] and triplet [207–209] excited dye molecules.

Semiconductor hetero-nanoparticles can be of considerable practical interest. The processes of charge separation in mixed CdS/TiO_2 semiconductor nanoparticles [79] and in the ZnO nanoparticle coated with a ZnS layer [210] are depicted schematically in Fig. 2. Production of large-bandgap hetero-nanoparticles can favour their spectral sensitisation. Additionally, as has been mentioned above, multicomponent nanoparticles are of interest, since it is possible to increase the efficiency of charge photoseparation because of the effective spatial separation of the electrons and holes in such structures. There are only a few experimental data [211, 212] on the photocatalytic acivity of hetero-nanoparticles analogous to those shown in Fig. 2. The possibility of increasing the quantum yield of charge separation in such hetero-nanoparticles has been demonstrated experimentally. In Fig. 17, the short-lived optical spectra of colloidal solutions of CdS and TiO_2 nanoparticles in CH_3CN generated by a laser pulse upon the excitation of CdS by light [58] are shown as an example. The short-lived optical absorption in the 500–750 nm region is caused by the electrons trapped by the Ti^{4+} centres of titanium dioxide. As can be seen from this picture, the excitation of CdS in CdS/TiO_2 nanoparticles leads to the electron transfer from CdS to TiO_2.

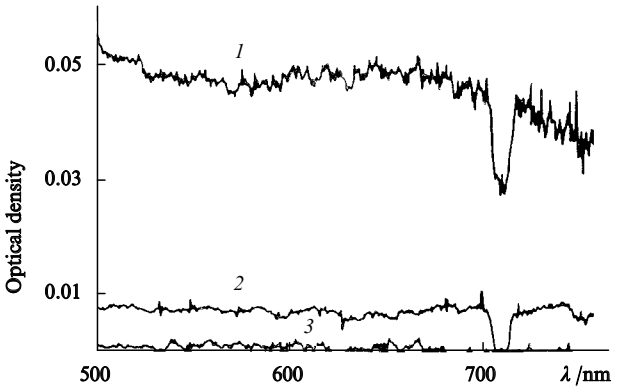


Figure 17. The absorption spectra of colloidal solutions of nanoparticles in CH_3CN after a laser pulse (λ = 355 nm, $\Delta\tau$ = 0 ps).
The concentration of nanoparticles in solution /mmol litre^{-1}: (*1*) 0.75(CdS) + 1.15(TiO_2); (*2*) 0.75(CdS); (*3*) 1.15(TiO_2).

The high photocatalytic activity of nanoparticles of the 'core–shell' type has been demonstrated in the example of the photooxidation of I^- and SCN^- anions by SnO_2/TiO_2 nanoparticles.[70] It was found that the quantum efficiency of the photooxidation of I^- anions by SnO_2/TiO_2 nanoparticles is 2–3 times higher than the quantum efficiency of the photooxidation by SiO_2/TiO_2 or TiO_2 nanoparticles. The use of systems of the 'core–shell' type is also promising in view of cutting the costs of hetero-nanoparticles if inexpensive materials are used for the synthesis of the cores for such structures.[63, 67, 71, 210, 213, 214]

2. Photocatalysis based on nanostructured films of semiconductors

Colloidal solutions of nanoparticles are suitable objects for the demonstration of the possibility of their use in photocatalysis. However, the practical use of colloidal solutions is difficult because of the need to separate nanoparticles from the solution after the completion of the photocatalytic process. Thin layers of nanoparticles adsorbed on a carrier seem to be much more promising, especially the films composed of hetero-nanoparticles shown in Fig. 3. These films have many advantages over films composed of nanoparticles of the same nature, namely, the expanded spectral sensitivity region of the large-bandgap semiconductor nanoparticles, increased quantum efficiency of charge photoseparation,[215] and high efficiency of spectral sensitisation of films by dyes.[216]

An idealised illustration of photocatalytic processes occurring on the surface of a conducting electrode with the participation of films composed of heteronanoparticles is exemplified in Fig. 3 with TiO_2/SnO_2 films. The position of the bottom of the SnO_2 conduction band is lower than that of the TiO_2 conduction band (0 and −0.5 V *vs.* NHE at pH 7, respectively). This causes the light-generated electrons to transfer from TiO_2 to SnO_2. The holes move in the opposite direction and are accumulated on the TiO_2 nanoparticles. As a result, an increase in the quantum efficiency of charge photoseparation and, hence, in the efficiency of the oxidation of donor molecules in solution can be observed in the structure under consideration. High efficiency of the TiO_2/SnO_2 film was demonstrated experimentally in the example of photocatalytic degradation of dyes (Acid Orange 7 and Naphthol Blue Black).[217, 218] The overall processes occurring at the anode and cathode can be described by the following scheme:
at the photoanode

$$SnO_2/TiO_2 + h\nu \longrightarrow [SnO_2(e^-...h^+)]/[TiO_2(e^-...h^+)] \longrightarrow$$
$$\longrightarrow SnO_2(e^-) + TiO_2(h^+),$$
$$TiO_2(h^+) + OH^- \longrightarrow TiO_2 + OH^{\bullet},$$
$$TiO_2(h^+) \text{ or } OH^{\bullet} + \text{dye} \longrightarrow \text{products};$$

at the cathode

$$Pt(2e^-) + O_2 + 2H^+ \longrightarrow H_2O_2.$$

Porous nanostructured films possess high adsorption capacity to organic dyes and organometallic compounds. Large specific surface area of such films allows adsorption of a considerable amount of a dye. The use of these properties of the nanostructured films makes it possible to increase substantially their photocatalytic efficiency due to sensitisation into the visible region.[72, 219]

V. Conclusion

Some interesting peculiarities in the solution behaviour of the ultrasmall semiconductor particles containing several hundreds of atoms have been revealed in the studies of their properties. Unusual physicochemical properties of semiconductor nanoparticles depend on three main factors. First, the size of nanoparticles is comparable with the molecular dimensions. This determines the difference between the kinetics of chemical transformations on the surface or in the bulk of nanoparticles and the kinetics of chemical transformations in infinite space. The classical equations of chemical kinetics can be used for the description of the processes on the surface of nanoparticles down to a size that exceeds the actual size of the reacting molecules by an order of magnitude. The processes occurring on the surface of smaller nanoparticles can be described by the Monte Carlo method or by the methods of stochastic kinetics.

Second, the surface atoms constitute a considerable proportion of the total number of atoms of a nanoparticle. This strongly affects the thermodynamic characteristics of nanoparticles and determines the size dependences of melting temperatures and pressures at which the crystal lattice of a semiconductor rearranges (*i.e.*, phase transition occurs).

And, finally, third, the non-linear optical effects arise and the energies of excitonic transitions in nanoparticles, oscillator strengths, and redox characteristics become dependent on the nanoparticle size as the latter becomes comparable with the delocalisation area of charge carriers.

Intensive investigations in the field of the chemistry of semiconductor nanoparticles have been carried out during the last decade. The major efforts of researchers are directed to the development of methods for the synthesis of nanostructures with controlled characteristics and investigation of their photocatalytic properties. Considerable progress has been achieved in the demonstration of the possibility of the use of semiconductor nanostructures for photocatalytic mineralisation of various environmentally hazardous compounds. In our opinion, the most promising lines in the study of semiconductor nanoparticles in the coming years will be associated with the development of methods for the synthesis of nanoparticles with predetermined geometric characteristics, studies of the mechanisms of chemical transformations at the liquid – solid interface in colloidal solutions of nanoparticles, practical implementation of nanoparticles and films produced on their basis in photocatalysis, and design of complex ordered systems for electronics.

This work has been written with the financial support by the Russian Foundation for Basic Research (Project No. 96-03-32360).

References

1. Al L Efros, A L Efros *Fiz. Tekh. Poluprovodn.* **16** 1209 (1982)
2. L E Brus *J. Chem. Phys.* **80** 4403 (1984)
3. A Henglein *Chem. Rev.* **89** 1861 (1989)
4. C R Berry *Phys. Rev.* **161** 848 (1967)
5. R Rossetti, J L Ellison, J M Gibson, L E Brus *J. Chem. Phys.* **80** 4464 (1984)
6. H Weller, U Koch, M Gutierrez, A Henglein *Ber. Bunsenges. Phys. Chem.* **88** 649 (1984)
7. N Herron, J C Calbrese, W E Farneth, Y Wang *Science* **259** 1426 (1993)
8. J Kuczynski, J K Thomas *J. Phys. Chem.* **87** 5498 (1983)
9. P Lianos, J K Thomas *Chem. Phys. Lett.* **125** 299 (1986)
10. C Petit, M P Pileni *J. Phys. Chem.* **92** 2282 (1988)
11. R R Chandler, J L Coffer *J. Phys. Chem.* **97** 9767 (1993)
12. Y Wang, W Mahler *Opt. Commun.* **61** 233 (1987)
13. Y Wang, A J Suna, J McHugh, E F Hilinski, P Lucas, R D Johnson *J. Chem. Phys.* **92** 6927 (1990)
14. W Mahler *Inorg. Chem.* **27** 435 (1988)
15. N F Borrelli, D W Hall, H J Holland, D W Smith *J. Appl. Phys.* **61** 5399 (1987)
16. B G Potter, J H Simmons *Phys. Rev. B, Condens. Matter* **37** 10838 (1988)
17. Y Wang, N Herron *J. Phys. Chem.* **91** 257 (1987)
18. Y Wang, N Herron *J. Phys. Chem.* **92** 4988 (1988)
19. N Herron, Y Wang, M Eddy, G D Sturky, D E Cox, K Molley, T Bein *J. Am. Chem. Soc.* **111** 530 (1989)
20. M W Peterson, M T Nenadovic, T Rajh, R Herak, O Micic, J P Goral, A J Nozik *J. Phys. Chem.* **92** 1400 (1988)
21. N A Rubtsova, R F Khairutdinov *Khim. Fiz.* **11** 502 (1992) [a]
22. K L Roberts, E J Markel *J. Phys. Chem.* **98** 4083 (1994)
23. M S El-Shall, W Slack, W Vann, D Kane, D Hanley *J. Phys. Chem.* **98** 3067 (1994)
24. M S El-Shall, D Graiver, U Pernisz, M I Baraton *Nanostruct. Mater.* **6** 297 (1995)
25. M S El-Shall, S Li, D Graiver, U Pernisz *Nanotechnology. Molecular Designed Materials (ACS Symp. Ser.)* **622** 79 (1996)
26. R I Bickley, T Gonzalez-Carreno, J S Lees, L Palmisano, R J D Tilley *J. Solid State Chem.* **82** 178 (1991)
27. J H Fendler *Isr. J. Chem.* **33** 41 (1993)
28. A Jentys, R W Grimes, J D Gale, C R A Catlow *J. Phys. Chem.* **97** 13535 (1993)
29. I Wilner, Y Eichen *J. Am. Chem. Soc.* **109** 6862 (1987)
30. N A Rubtsova, R F Khairutdinov, S M B Kosta *Kolloid. Zh.* **55** 144 (1993) [b]
31. L Spanhel, M Haase, H Weller, A Henglein *J. Am. Chem. Soc.* **109** 5649 (1987)
32. T Dannhauser, M O'Neil, K Johansson, D Witten, G McLendon *J. Phys. Chem.* **90** 6074 (1986)
33. A Henglein *Top. Curr. Chem.* **143** 113 (1988)
34. I G Dance, A Choy, M L Scudder *J. Am. Chem. Soc.* **106** 6285 (1984)
35. M L Steigerwald, A P Alivisatos, J M Gibson, T D Harris, R Kortan, A J Muller, A M Thayer, T Duncan, M Douglass, L E Brus *J. Am. Chem. Soc.* **110** 3046 (1988)
36. Y Nosaka, K Yamaguchi, H Hayashi *Chem. Lett.* 605 (1988)
37. C -H Fischer, A Henglein *J. Phys. Chem.* **93** 5578 (1989)
38. V Swayambunathan, D H Hayes, K Schmidt, Y X Liao, D Meisel *J. Am. Chem. Soc.* **112** 3831 (1990)
39. Y Wang, M Harmer, N Herron *Isr. J. Chem.* **33** 31 (1993)
40. H Weller, A Eychmuller, R Vogel, L Katsikas, A Hasselbarth, M Giersig *Isr. J. Chem.* **33** 107 (1993)
41. P V Kamat *CHEMTECH* 22 (1995)
42. G D Stucky, J E McDougall *Science* **247** 669 (1990)
43. H Krautscheid, D Fenske, G Baum, M Semmelmann *Angew. Chem., Int. Ed. Engl.* **32** 1303 (1993)
44. T Vossmeyer, G Reck, L Katsakas, E Haupt, B Schulz, H Weller *Science* **267** 1476 (1995)
45. M L Steigerwald *Polyhedron* **13** 1245 (1993)
46. N Herron, Y Wang, H Eckert *J. Am. Chem. Soc.* **112** 1322 (1990)
47. C B Murray, D B Norris, M G Bawendi *J. Am. Chem. Soc.* **115** 8706 (1993)
48. Y Wang, N Herron *J. Phys. Chem.* **95** 525 (1991)
49. A P Alivisatos *Mater. Res. Soc. Bull.* **20** 23 (1995)
50. J J Shiang, A Kadavanich, R K Grubbs, A P Alivisatos *J. Phys. Chem.* **99** 17417 (1995)
51. C J Sandorf, D M Hwang, W M Chung *Phys. Rev. B, Condens. Matter* **33** 5953 (1986)
52. E Matijevic *Annu. Rev. Mater. Sci.* **15** 483 (1986)
53. R D Stramel, J K Thomas *J. Colloid Interface Sci.* **110** 121 (1986)
54. R F Khairutdinov, N A Rubtzova, S M B Costa *J. Lumin.* **68** 293 (1996)
55. M Visca, E Matijevic *J. Colloid Interface Sci.* **68** 308 (1979)
56. A Fojtik, H Weller, S Fiechler, A Henglein *Chem. Phys. Lett.* **134** 477 (1987)
57. L Spanhel, H Weller, A Henglein *J. Am. Chem. Soc.* **109** 6632 (1987)
58. K R Gopidas, M Bohorquez, P V Kamat *J. Phys. Chem.* **94** 6435 (1990)
59. N Serpone, E Borgarello, M Grätzel *J. Chem. Soc., Chem. Commun.* 342 (1984)
60. R Vogel, P Hoyer, H Weller *J. Phys. Chem.* **98** 3183 (1994)
61. S Hotchandani, P V Kamat *J. Phys. Chem.* **96** 6834 (1992)
62. P V Kamat, I Bedja, S Hotchandani, L K Patterson *J. Phys. Chem.* **100** 4900 (1996)
63. A Haesselbarth, A Eychmueller, R Eichberger, M Giersig, A Mews, H Weller *J. Phys. Chem.* **97** 5333 (1993)
64. L Spanhel, A Henglein, H Weller *Ber. Bunsenges. Phys. Chem.* **91** 1359 (1987)
65. A Henglein, M Gutierrez, H Weller, A Fojtik, J Jirkowsky *Ber. Bunsenges. Phys. Chem.* **93** 593 (1989)
66. A J Nozik *Appl. Phys. Lett.* **30** 567 (1977)
67. A R Kortan, R Hull, R L Opila, D A Stams, T D Thomas, D C McLaren, De Ji, T H Morton *J. Am. Chem. Soc.* **112** 1327 (1990)
68. P V Kamat, B Patrick *J. Phys. Chem.* **96** 6829 (1992)
69. J Rabani *J. Phys. Chem.* **93** 7707 (1989)
70. I Bedja, P V Kamat, *J. Phys. Chem.* **99** 9182(1995)
71. M Ocana, W P Hsu, E Matijevic *Langmuir* **7** 2911 (1991)
72. I Bedja, S Hotchandani, P V Kamat *J. Phys. Chem.* **98** 4133 (1994)
73. H K Yoshiki, A Fujishima *J. Electrochem. Soc.* **142** 428 (1995)
74. B O'Regan, M Grätzel, D Fitzmaurice *Chem. Phys. Lett.* **183** 89 (1991)
75. L Kavan, B Oregan, A Kay, M Grätzel *J. Electroanal. Chem.* **346** 291 (1993)
76. I Bedja, S Hotchandani, P V Kamat *J. Phys. Chem.* **97** 11064 (1993)
77. U Bjorksten, J Moser, M Grätzel *Chem. Mater.* **6** 858 (1994)
78. L Kavan, T Stoto, M Grätzel, D Fitzmaurice, V Shklover *J. Phys. Chem.* **97** 9493 (1993)
79. R Vogel, K Pohl, H Weller *Chem. Phys. Lett.* **174** 241 (1990)
80. A T Bharucha-Reid *Elements of the Theory of Markov Processes and Their Applications* (New York: McGraw-Hill, 1960)
81. D A McQuarrie *J. Chem. Phys.* **38.** 433 (1963)
82. D A McQuarrie, C J Jachimowski, M E Russell *J. Chem. Phys.* **40** 2914 (1964)
83. G Rothenberger, P P Infelta, M Grätzel *J. Phys. Chem.* **85** 1850 (1981)

84. R F Khairutdinov, N Serpone *Prog. React. Kinet.* **21** 1 (1996)
85. R F Khairutdinov, K Ya Burshtein, N Serpone *Photochem. Photobiol. A: Chem.* **98** 1 (1996)
86. R F Khairutdinov, P P Levin, S M B Costa *Langmuir* **12** 714 (1996)
87. R F Khairutdinov, K I Zamaraev, V P Zhdanov *Electron Tunnelling in Chemistry*; *Comprehensive Chemical Kinetics* Vol. 33 (Amsterdam: Elsevier, 1988)
88. J Jortner, S Choi, J L Katz, S A Rice *Phys. Rev. Lett.* **11** 323 (1963)
89. R F Khairutdinov, K Ya Burshtein, N Serpone *Khim. Fiz.* **16** 2030 (1997) [a]
90. A Henglein *Prog. Colloid Polym. Sci.* **73** 1 (1987)
91. H Weller *Adv. Mater.* **5** 88 (1993)
92. H Weller, H M Schmidt, U Koch, A Fojtik, S Baral, A Henglein, W Kunath, K Weiss, E Dieman *Chem. Phys. Lett.* **124** 557 (1986)
93. O I Micic, T Rajh, J M Nedeljkovic, M I Comor *Isr. J. Chem.* **33** 59 (1993)
94. R A Hobson, P Mulvaney, F J Grieser *Chem. Soc., Chem. Commun.* 823 (1994)
95. E S Smotkin, C Lee, A J Bard, A Campion, M A Fox, T E Malouk, S E Webber, J M White *Chem. Phys. Lett.* **152** 265 (1988)
96. L Spanhel, M A Anderson *J. Am. Chem. Soc.* **112** 2278 (1990)
97. T Rajh, M I Vucemilovic, N M Dimitrijevic, O Micic, A J Nozik *Chem. Phys. Lett.* **143** 305 (1988)
98. D Hayes, D Meisel, O I Micic *Colloids Surf.* **55** 121 (1991)
99. L Brus *J. Phys. Chem.* **90** 2555 (1986)
100. Yu I Petrov *Fizika Malykh Chastits* (The Physics of Small Particles) (Moscow: Nauka, 1982)
101. M L Steigerwald, L E Brus *Acc. Chem. Res.* **23** 183 (1990)
102. M V Ramakrishna, R A Friesner *J. Chem. Phys.* **95** 8309 (1991)
103. Y Nosaka, N Ohta, H Miyama *J. Phys. Chem.* **94** 3752 (1990)
104. R Rosetti, R Hull, J M Gibson, L E Brus *J. Chem. Phys.* **83** 1406 (1985)
105. A I Ekimov, A A Onushchenko *Pis'ma Zh. Eksp. Teor. Fiz.* **40** 337 (1984)
106. T Rajh, M W Peterson, J A Turner, A J Nozik. *J. Electroanal. Chem. Interfacial Electrochem.* **228** 55 (1987)
107. H Weller, M Haase, L Spanhel, A Henglein *Prog. Colloid Polym. Sci.* **76** 24 **(**1988)
108. D M Mittleman, R W Schoenlein, J J Shiang, V L Colvin, A P Alivisatos, C V Shank *Phys. Rev. B, Condens. Matter* **49** 14435 (1994)
109. R S Knox *Theory of Excitons* (New York: Academic Press, 1963)
110. Y Kayanuma *Phys. Rev. B, Condens. Matter* **38** 9797 (1988)
111. P E Lippens, M Lannoo *Phys. Rev. B, Condens. Matter* **39** 10935 (1989)
112. P E Lippens, M Lannoo *Phys. Rev. B, Condens. Matter* **41** 6079 (1990)
113. Y Wang, A Suna, W Mahler, R Kasowski *J. Chem. Phys.* **87** 7315 (1987)
114. W J Albery, G T Brown, J R Darwent, E Saivar-Iranizad *J. Chem. Soc., Faraday Trans. 1* **81** 1999 (1985)
115. J P Kuczynski, B H Milosavljevic, J K Thomas *J. Phys. Chem.* **88** 980 (1984)
116. C Liu, A J Bard *J. Phys. Chem.* **93** 3232 (1989)
117. U Koch, A Fojtik, H Weller, A Henglein *Chem. Phys. Lett.* **122** 507 (1988)
118. D Bahnemann, C Kormann, M R Hoffmann *J. Phys. Chem.* **91** 3789 (1987)
119. A Henglein, A Kumar, E Janata, H Weller *Chem. Phys. Lett.* **132** 133 (1986)
120. A V Barzykin, M A Fox *Isr. J. Chem.* **33** 21 (1993)
121. M Haase, H Weller, A Henglein *J. Phys. Chem.* **92** 482 (1988)
122. T S Moss *Proc. Phys. Soc. London, B* **67** 775 (1954)
123. B E Burstein *Phys. Rev.* **93** 632 (1954)
124. E Hilinski, P Lucas, Y Wang *J. Chem. Phys.* **89** 3435 (1988)
125. W G Becker, A J Bard *J. Phys. Chem.* **87** 4888 (1983)
126. H C Youn, S Baral, J H Fendler *J. Phys. Chem.* **92** 6320 (1988)
127. M F Finlayson, K H Park, N Kakuta, A J Bard, A Campion, M A Fox, S E Webber, J M White *J. Lumin.* **39** 205 (1988)
128. A Fojtik, H Weller, U Koch, A Henglein *Ber. Bunsenges. Phys. Chem.* **88** 969 (1984)
129. Y M Tricot, J H Fendler *J. Phys. Chem.* **90** 3369 (1986)
130. R D Stramel, T Nakamura, J K Thomas *J. Chem. Soc., Faraday Trans.* **84** 1287 (1988)
131. P V Kamat, N M Dimitrijevic, R W Fessenden *J. Phys. Chem.* **91** 396 (1987)
132. K R Gopidas, P V Kamat *Proc. Indian Acad. Sci. Chem. Sci.* **105** 505 (1993)
133. A I Ekimov, I A Kudryavtsev, M G Ivanov, A L Efros *J. Lumin.* **46** 83 (1990)
134. M Haase, H Weller, A Henglein *J. Phys. Chem.* **92** 4706 (1988)
135. T Rajh, O I Micic, D Lawless, N Serpone *J. Phys. Chem.* **96** 4633 (1992)
136. Y Nosaka, K Tanaka, N Fujii *J. Appl. Polym. Sci.* **47** 1773 (1993)
137. K R Gopidas, P V Kamat *Mater. Lett.* **9** 372 (1990)
138. N M Dimitrijevic *J. Chem. Soc., Faraday Trans.* **83** 1193 (1987)
139. N Chestnoy, T D Harris, R Hull, L E Brus *J. Phys. Chem.* **90** 3393 (1986)
140. T Takagahara *Phys. Rev. B, Condens. Matter* **36** 9293 (1987)
141. E Hanamura *Phys. Rev. B, Condens. Matter* **37** 1273 (1988)
142. E Hanamura *Phys. Rev. B, Condens. Matter* **38** 1228 (1988)
143. T Itoh, M Furumiya, T Ikehara *Solid State Commun.* **73** 272 (1990)
144. T Rajh, O I Micic, A J Nozik *J. Phys. Chem.* **97** 11999 (1993)
145. P Siders, R A Marcus *J. Am. Chem. Soc.* **103** 741 (1981)
146. J Jortner *J. Chem. Phys.* **64** 4860 (1976)
147. C K Mann, K K Barnes *Electrochemical Reactions in Nonaqueous Systems* (New York: Marcel Dekker, 1970)
148. H Harada, T Ueda, T Sakata *J. Phys. Chem.* **93** 1542 (1989)
149. J Chrysochoos *J. Phys. Chem.* **96** 2868 (1992)
150. A N Goldstein, C M Echer, A P Alivisatos *Science* **256** 1425 (1992)
151. S H Tolbert, A P Alivisatos *Science*,**265** 373 (1994)
152. M Haase, A P Alivisatos *J. Phys. Chem.* **96** 6756 (1992)
153. A P Alivisatos *J. Phys. Chem.* **100** 13226 (1996)
154. L E Brus, W A Goddard, A Kaldor, S G Louie, M Moscovitz, P S Peercy *Chem. Eng. News* **70** 18 (1992)
155. R Dagani *Chem. Eng. News* 18 (1992)
156. S T Martin, H Herrmann, W Choi, M R Hoffmann *J. Chem. Soc., Faraday Trans.* **90** 3315 (1994)
157. A Henglein *J. Phys. Chem.* **86** 2291 (1982)
158. D Duonghong, J Ramsden, M Grätzel *J. Am. Chem. Soc.* **104** 2877 (1982)
159. A Harriman, G Porter, P Walters *J. Photochem.* **19** 183 (1982)
160. D Bahnemann, A Henglein, L Spanhel *Faraday Discuss. Chem. Soc.* **78** 151 (1984)
161. G T Brown, J R Darwent, P D Fletcher *J. Am. Chem. Soc.* **107** 6446 (1985)
162. G Rothenberger, J Moser, M Grätzel, N Serpone, D K Sharma *J. Am. Chem. Soc.* **107** 8054 (1985)
163. N Serpone, D K Sharma, J Moser, M Grätzel *Chem. Phys. Lett.* **136** 47 (1987)
164. J A Navio, F J Marchena, M Roncel, M A De la Rosa *J. - Photochem. Photobiol. A: Chem.* **55** 319 (1991)
165. I Willner, Y Eichen, A J Frank, M A Fox *J. Phys. Chem.* **97** 7264 (1993)
166. X Liu, K K Iu, J K Thomas *J. Chem. Soc., Faraday Trans.* **89** 1861 (1993)
167. J J Ramsden, M Grätzel *Chem. Phys. Lett.* **132** 269 (1986)
168. P V Kamat, N M Dimitrijevic, R W Fessenden *J. Phys. Chem.* **92** 2324 (1988)
169. P V Kamat, N M Dimitrijevic *Proc. Electrochem. Soc.* **6** 90 (1988)
170. A Green, A Mills *J. Photochem. Photobiol. A: Chem.* **64** 211 (1992)
171. P V Kamat *J. Photochem.* **28** 513 (1985)
172. P V Kamat *J. Chem. Soc., Faraday Trans.* **81** 509 (1985)
173. K R Gopidas, P V Kamat *J. Phys. Chem.* **93** 6428 (1989)
174. B Patrick, M V George, P V Kamat, S Das, K G Thomas *J. Chem Soc., Faraday Trans.* **88** 671 (1992)
175. K Vinodgopal, I Bedja, S Hotchandani, P V Kamat *Langmuir* **10** 1767 (1994)
176. B Kraeutler, A J Bard *J. Am. Chem. Soc.* **100** 2239 (1978)
177. B Kraeutler, C D Jaeger, A J Bard *J. Am. Chem. Soc.* **100** 4903 (1978)
178. B Kraeutler, A J Bard *Nouv. J. Chim.* **3** 331 (1979)
179. H Al-Ekabi, P De Mayo *J. Phys. Chem.* **89** 5815 (1985)
180. T Hasegawa, P De Mayo *Langmuir* **2** 362 (1986)
181. M A Fox *Top. Curr. Chem.* **142** 72 (1987)

182. M A Fox, in *Advances in Electron Transfer Chemistry* Vol. 1 (Ed. P S Mariano) (Greenwich: Jai Press, 1991) p. 1
183. J Moser, M Grätzel *Helv. Chim. Acta* **65** 1435 (1982)
184. D J Fitzmaurice, M Eschle, H Frei, J E Moser *J. Phys. Chem.* **97** 3806 (1993)
185. N Serpone, D Lawless, R F Khairutdinov, E Pelizzetti. *J. Phys. Chem.* **99** 16655 (1995)
186. P V Kamat, N M Dimitrijevic *J. Phys. Chem.* **93** 4259 (1989)
187. G T Brown, J R Darwent *J. Phys. Chem.* **88** 4955 (1984)
188. W G Becker, M M Truong, C C Ai, N N Hamel *J. Phys. Chem.* **93** 4882 (1989)
189. R C Schiek, in *Kirk-Othmer Encyclopedia of Chemical Technology* Vol. 17 (Eds R E Kirk, D F Othmer, M Grayson, D Eckroth) (New York: Wiley, 1982) p. 788
190. J S Connolly (Ed.) *Photochemical Conversion and Storage of Solar Energy* (New York: Academic Press, 1981)
191. M Grätzel (Ed.) *Energy Resources through Photochemistry and Catalysis* (New York: Academic Press, 1983)
192. D F Ollis, E H Al (Eds) *Photocatalytic Purification and Treatment of Water and Air* (Amsterdam: Elsevier, 1993)
193. M A Fox, M T Dulay *Chem. Rev.* **93** 341 (1993)
194. M R Hoffmann, S T Martin, W Choi, D W Bahnemann *Chem. Rev.* **95** 95 (1995)
195. K Rajeshwar *J. Appl. Electrochem.* 25 (1995)
196. N Serpone, R F Khairutdinov, in *Nanocrysalline Semiconductor Materials* (Eds P V Kamat, D Meisel) (Amsterdam: Elsevier, 1996)
197. R Baba, S Nakabayashi, A Fujishima, K Honda *J. Phys. Chem.* **89** 1902 (1985)
198. R Palmans, A J Frank *J. Phys. Chem.* **95** 9438 (1991)
199. K Kalyanasundaram, E Borgarello, M Grätzel *Helv. Chim. Acta* **64** 362 (1981)
200. Y F Lee, M Olshavsky, J Chrysochoos *J. Less-Common Met.* **148** 259 (1989)
201. S C Martin, C L Morrison, M R Hoffmann *J. Phys. Chem.* **98** 13695 (1994)
202. P V Kamat *Prog. React. Kinet.* **19** 277 (1994)
203. R Rossetti, L E Brus *J. Am. Chem. Soc.* **106** 4336 (1984)
204. P V Kamat, K R Gopidas, D Weir *Chem. Phys. Lett.* **149** 491 (1988)
205. S Umapathy, A M Cartner, A W Parker, R E Hester *J. Phys. Chem.* **94** 8880 (1990)
206. P V Kamat, S Das, K G Thomas, M V George *Chem. Phys. Lett.* **178** 75 (1991)
207. M A Ryan, E C Fitzgerald, M T Spitler *J. Phys. Chem.* **93** 6150 (1989)
208. B Patrick, P V Kamat *J. Phys. Chem.* **96** 1423 (1992)
209. A Kay, R Humphry-Backer, M Grätzel *J. Phys. Chem.* **98** 952 (1994)
210. A Eychmuller, T Vobmeyer, A Mews, H Weller *J. Lumin.* **58**. 223 (1994)
211. N Serpone, E Borgarello, M Grätzel *J. Chem. Soc., Chem. Commun.* 319 (1984)
212. N Serpone, P Maruthamuthu, P Pichat, E Pelizzetti, H Hidaka *J. Photochem. Photobiol. A: Chem.* **85** 247 (1995)
213. J W Haus, H S Zhou, I Honma, H Komiyama *Phys. Rev. B, Solid State, Ser. 3* **47** 1359 (1993)
214. H S Zhou, I Honma, H Komiyama, J W Haus *J. Phys. Chem.* **97** 895 (1993)
215. D Liu, P V Kamat *J. Phys. Chem.* **97** 10769 (1993)
216. S Hotchandani, P V Kamat *Chem. Phys. Lett.* **191** 320 (1992)
217. K Vinodgopal, P V Kamat *Environ. Sci. Technol.* **29** 841 (1985)
218. K Vinodgopal, I Bedja, P V Kamat *Chem. Mater.* **8** 2180 (1996)
219. A Kay, M Grätzel *J. Phys. Chem.* **97** 6272 (1993)

[a] — *Russ. J. Chem. Phys. (Engl. Transl.)*
[b] — *Colloid J. (Engl. Transl.)*